SAND2017-3298R

Error Analysis of CM Data Products Input Distributions

Brian Hunt[1], Lainy Cochran[1], Aubrey Eckert-Gallup[2], Terry Kraus[1], Mark Allen[3], Sean Fournier[3]

Departments 6631[1], 6233[2], and 4131[3]
Sandia National Laboratories
P.O. Box 5800
Albuquerque, New Mexico 87185-0748

Colin Okada

National Security Technologies, Remote Sensing Laboratory
Contractor to US Department of Energy
P.O. Box 98521, M/S RSL-47
Las Vegas, Nevada 89193-8521

Matthew Simpson

Lawrence Livermore National Laboratory
National Atmospheric Release Advisory Center
P.O. Box 808, L-103
Livermore, California 94551

CONTENTS

FIGURES

TABLES

ACKNOWLEDGMENTS

Sandia National Laboratories is a multi-mission laboratory managed and operated by Sandia Corporation, a wholly owned subsidiary of Lockheed Martin Corporation, for the U.S. Department of Energy's National Nuclear Security Administration under contract DE-AC04-94AL85000.

1 INTRODUCTION

This goal of this project is to address the current inability to assess the overall error and uncertainty of data products developed and distributed by DOE's Consequence Management (CM) Program. This is a widely recognized shortfall, the resolution of which would provide a great deal of value and defensibility to the analysis results, data products, and the decision making process that follows this work. A global approach to this problem is necessary because multiple sources of error and uncertainty contribute to the ultimate production of CM data products. Therefore, this project will require collaboration with subject matter experts across a wide range of FRMAC skill sets in order to quantify the types of uncertainty that each area of the CM process might contain and to understand how variations in these uncertainty sources contribute to the aggregated uncertainty present in CM data products. The ultimate goal of this project is to quantify the confidence level of CM products to ensure that appropriate public and worker protections decisions are supported by defensible analysis.

This project seeks to develop a probabilistic framework to characterize the CM process and the interrelated nature of error and uncertainty propagation that contributes to the overall uncertainty in CM data products. This framework will be developed for a single CM data product that will serve as a proof of concept. The first step of this work identified the sources of error and uncertainty for this specific data product. The second step of this work is to characterize these sources of error and uncertainty using probability distributions. The purpose of this report is to describe the derivation of probability distributions for the sources of error and uncertainty that have been identified thus far.

This scope of this TI project is limited to the analysis of the uncertainty associated with Public Protection Derived Response Levels (DRLs), which are used to evaluate the radiological impacts to members of the public from exposure to radioactive material. A Derived Response Level (DRL) is a level of radioactivity in the environment that would be expected to produce a dose equal to the corresponding Protective Action Guide (PAG). The CM data products for which Public Protection DRLs are calculated are used to help decision makers determine where protective actions (e.g., sheltering, evacuation, or relocation of the public) may be warranted.

To create a finished product, ready for distribution to decision makers, health physics calculations are performed using Turbo FRMAC to estimate the likely dose that may be received by the public following a radiological release. These calculations rely on data which may be collected from one of several methods: analytical results from laboratories, results from Aerial Measurement Systems, or field measurements made by ground-based monitoring teams. Results of the calculations are then applied to create contours on a data grid developed using NARAC plume predictions.

The goal of this analysis is to characterize uncertainty in the CM data product development process. This does not require the characterization of uncertainty inherent to the situation under analysis; sources of uncertainty such as the type of release, location of release, weather, etc., will be held constant for this project in order to allow for the examination of the impact of sources of uncertainty within the analysis process itself. A demonstration scenario has been selected for this analysis with the following characteristics:

- Detonation of an Cs-137 RDD on level terrain within a stable wind class
- Particles created by the detonation are all 1 μm diameter.
- Source term of sufficient quantity to create a deposition of 330 $\mu Ci/m^2$ at a location downwind

The following sections describe the probability distribution defined for the sources of error and uncertainty identified in each portion of the CM analysis process. Calculation inputs that contribute to uncertainty in the health physics calculations of Public Protection DRLs are described and assigned probability distributions in Section 2. Probability distributions for sources of uncertainty in data collection are given in Section 3. The distributions developed to characterize possible sources of uncertainty in NARAC plume predictions are given in Section 4.

2 PUBLIC PROTECTION DRL INPUT UNCERTAINTY DISTRIBUTIONS

In determining the distributions for the Public Protection DRL inputs, the original reference for each input was examined for uncertainty information. In the case that uncertainty information was not available in those documents, additional references were sought out. The RESRAD probabilistic analyses and U.S. Nuclear Regulatory Commission (NRC) State-of-the-Art Reactor Consequence Analysis (SOARCA) uncertainty analyses were also examined as potential sources of uncertainty information because those analyses have many inputs that are the same or similar to those used in the FRMAC assessment methods.

For details on the inputs described in the following sections, refer to Method 1.1 in the FRMAC Assessment Manual [1].

2.1 Deposition (*Dp*) or Integrated Air Activity ($\tilde{A}$)

Sections 3 and 4 include uncertainty information for Deposition and Integrated Air Activity. In a typical response, mixture information is initially provided by atmospheric modeling (NARAC) and eventually informed by field and laboratory measurements. For purposes of this analysis, mixtures and associated uncertainties from NARAC, Monitoring & Sampling, and Laboratory Analysis will be treated as separate mixture inputs.

2.2 Deposition Velocity (V_d)

Deposition velocity is the rate at which airborne material is deposited on the ground. Turbo FRMAC uses deposition velocity to convert between Integrated Air Activity and Deposition. All deposition is assumed to be dry particulates. Wet deposition is not included in FRMAC Assessment methods.

The FRMAC default deposition velocity for particulates is 0.3 cm/s. NUREG/CR-4551 Vol. 2 Rev. 1 Part 7 [2] provides a deposition velocity uncertainty for the NRC assessment of risks from severe accidents for five U.S. nuclear power plants, as detailed in NUREG-1150. The recommended dry deposition velocity range was 0.03 cm/s to 3.0 cm/s with a most likely value of 0.3 cm/s, in agreement with the FRMAC default. The range accounts for uncertainty in particle size, wind speed, surface roughness, and aerosol density, and is intended to be applicable for a residential suburb (i.e., roads, lawns, and trees). A triangular distribution with this range and a mode of 0.3 cm/s will be used for this analysis.

2.3 Breathing Rates (BR_{AA}, BR_{LE})

This initial analysis is limited to the Adult Whole Body age group and organ (FRMAC default assumption) and thus concerns adult breathing rates and activity times. Turbo FRMAC calculates breathing rates by activity, using activity time and activity-specific breathing rate inputs. The activity-specific breathing rates used by FRMAC are taken from ICRP 66 Table B.15 [3]. A Light-Exercise Breathing Rate (BR_{LE}) of 1.5 m^3/h is used for in-plume inhalation. An Activity-Averaged Breathing Rate (BR_{AA}) of 0.92 m^3/h is used for inhalation of resuspended material. The activity times used to calculate BR_{AA} are shown in Table 1.

Table 1. FRMAC Defaults for Adult Male

Activity	Time (h)	Breathing Rate (m^3/h)
Sleeping	8.50	0.45
Sitting	5.50	0.54
Light Exercise	9.75	1.50
Heavy Exercise	0.25	3.00
Total	24	--

A distribution is needed for BR_{LE} by itself, and for either each activity-specific breathing rate or the overall BR_{AA}. The time budgeted for each activity is assumed to be fixed and will not be assigned an uncertainty.

ICRP 66

The discrete values for respiratory frequency, tidal volume, and minute ventilation provided in ICRP 66, Table B.15 as a function of age, gender, and activity level do not include any information about associated error. It is difficult to determine the exact source of these values in the provided references.

ICRP 66 does provide transformations for exercise that relate vital capacity to tidal volume at a respiratory frequency of 30 min^{-1} and at maximal value. It also includes relationships between tidal volume at a respiratory frequency of 30 min^{-1} and minute ventilation (i.e., breathing rate). This analysis of FRMAC methods needs to be able to distinguish between light and heavy exercise, and unfortunately the relationships based on a fixed respiratory frequency of 30 min^{-1} given in ICRP 66 do not allow for this distinction.

RESRAD

The developers of RESRAD provide triangular distributions for "residential" and "building occupancy" inhalation rates [4]. These distributions account for variation in activity level, gender, and age. The RESRAD approach could possibly be used for the overall BR_{AA}, rather than applying distributions to each activity-specific breathing rate. For example, the RESRAD residential breathing rate distribution uses an activity-averaged breathing rate of 23 m^3/d (0.96 m^3/h) as the mode, a sedentary breathing rate of 0.5 m^3/h as the minimum, and a moderate activity breathing rate of 1.5 m^3/h as the maximum. A similar distribution is developed for this analysis using the FRMAC default activity-specific breathing rates for sitting (0.54 m^3/h) as the minimum, light exercise (1.5 m^3/h) as the maximum, and the default BR_{AA} (0.92 m^3/h) as the mode.

EPA Exposure Factors Handbook

The 2011 EPA Exposure Factors Handbook (EFH) [5] contains descriptive statistics on short-term gender-, age-, and activity-specific inhalation rates. This information has been used to develop a distribution for BR_{LE}. Table 6-17 of the EFH provides information for males performing "moderate intensity" activities, specifically. The "moderate intensity" activity level will be used for this analysis because it is most comparable to the FRMAC default BR_{LE}. The "21 to <30" age group was selected for this analysis because the BR_{LE} of 1.5 m^3/h used by default by FRMAC is cited as for a 30-year old male in Table B.15 of ICRP 66.

Table 6-17 of the EFH gives the mean and quantiles for the desired BR_{LE} distribution, hereafter referred to as the empirical BR_{LE} distribution. A truncated normal distribution was fit to this empirical distribution. This normal distribution uses the mean of 2.92e-2 m^3/minute (1.75 m^3/h) provided for the empirical distribution of BR_{LE}. The standard deviation for this distribution was calculated to minimize the root mean square error (RMSE) of the hypothesized normal distribution compared to the empirical distribution for the input, resulting in a standard deviation value of 7.00e-3 m^3/minute (0.42 m^3/h). A Komolgorov-Smirnov test was used to confirm that this distribution and its fitted parameters are appropriate for BR_{LE}. The minimum of the truncated normal BR_{LE} distribution is 9e-3 m^3/minute (0.54 m^3/h), the default FRMAC value for Adult Male sitting breathing rate, while the maximum is 5e-2 m^3/minute (3.0 m^3/h), the default FRMAC value for Adult Male heavy exercise breathing rate.

2.4 Deposition External Dose Coefficient (*Dp_ExDC*)

Eckerman recommends a multiplicative uncertainty for ground plane dose rate coefficients for all radionuclides and organs [6]. This multiplier is given a triangular distribution with a mode of 0.8, minimum of 0.5, and maximum of 1.5. This distribution is used by the NRC in their SOARCA uncertainty analyses [7] and will be applied for the purposes of the analysis described in this report.

2.5 Ground Roughness Factor (*GRF*)

The Deposition External Dose Coefficients used by FRMAC were calculated under the assumption that the radionuclides are deposited on an infinite flat plane. A Ground Roughness Factor (GRF) is used to account for the fact that this assumption is an approximation of reality. The default GRF used in FRMAC Assessment calculations is 0.82. This value is taken from Anspaugh et al. as specified in the equation for weathering [8]. A reference from the Anspaugh document by Likhtarev et al. states that "the initial migration or soil-roughness effect is taken into account by the factor 0.82 (which is the ratio of external gamma-exposure rate (EGER) in air due to Cs-137 source with a relaxation depth of 1 mm to that from an infinite plane source)" [9]. No uncertainty information is given in the Likhtarev document for this value.

Likhtarev cites Beck [10] for its cesium EGER (g_s) values: "Because only dry deposition occurred in Ukraine during April-May 1986, for all radionuclides except cesium values of g_s were used that are appropriate for an initial migration into soil that can be described by an exponential decrease in concentration with depth with a relaxation depth of 1 mm and a soil density of 1.6 g/cm^3." This depth corresponds to a relaxation length of 0.16 g/cm^2. Using the tables in Beck, this corresponds to a g_s ratio of 0.16 g/cm^2 to "plane" of 0.87. Beck estimates that "the majority of the conversion factors given…are accurate to ±5-10% for locations meeting the criteria of uniform deposition over an approximately 10-meter radius from the point of measurement for reasonably flat soil surfaces." In summary, uncertainty in the GRF is most likely driven by uncertainty in transport calculations and laboratory and field measurements. An uncertainty of 10% is assumed for purposes of this analysis. A distribution type is not specified by Beck, so a normal distribution is assumed.

SOARCA

The MELCOR Accident Consequence Code System (MACCS) used for SOARCA includes a variable called "GSHFAC" which is a groundshine shielding factor [11]. GSHFAC is "a multiplier on the value of groundshine dose that would have been received if the person were standing outside and the ground were a perfectly flat surface. A value of 0 indicates complete shielding from groundshine; a value of 1 indicates no protection." The SOARCA Sequoyah uncertainty analysis

[7] provides a distribution for GSHFAC which is combined with GSDE, "a dimensionless scaling factor used to account for the amount of ionizing radiation energy deposited within various human organs from external radiation emanating from the ground." The GSDE used for the SOARCA Sequoyah uncertainty analysis is the multiplicative uncertainty provided by Eckerman for ground plane dose rate coefficients (see Deposition External Dose Coefficient).

The distribution for GSHFAC accounts for uncertainties due to "indoor residence time, household shielding value, and departures from the infinite flat plane." The default FRMAC assumption for the receptor is that they are "outside in the contaminated area continuously during the time phase under consideration without any protective measures (e.g., shielding or respiratory protection)." Therefore, it is not appropriate to apply the GSHFAC distribution to GRF.

2.6 Inhalation Dose Coefficient (*InhDC*)

Eckerman recommends log-normal distributions for radionuclide- and organ-specific inhalation dose coefficients [6]. For Cs-137 Type F (Most Likely), a geometric standard deviation (GSD) of 1.50 is given for leukemia, bone, breast, thyroid, liver, colon, and residual. A GSD of 1.55 is given for lung. This distribution (truncated long-normal using 90% confidence interval as upper and lower values) was used for the SOARCA uncertainty analyses. An effective dose coefficient was not included in SOARCA because MACCS was used to calculate dose to the specific organs (cancer sites) previously listed. In a conversation with Eckerman on March 20, 2017, he recommended using a GSD of 1.50 for the Cs-137 effective dose coefficient. The committed effective dose coefficient for Cs-137 Type F (Most Likely) is 17.3 mrem/µCi and will be used as the mean.

2.7 Resuspension Factor (*K*)

The Resuspension Factor used by FRMAC comes from Maxwell and Anspaugh [12]. Maxwell and Anspaugh provide an uncertainty estimate of $4.2^{\pm 1}$, to be interpreted as a GSD. The GSD is to be applied to the entire Resuspension Factor, as shown in the equation below.

$$S_f = [10^{-5} \exp(-0.07t) + 7 \times 10^{-9} \exp(-0.002t) + 10^{-9}] \times 4.2^{\pm 1}$$

2.8 Protective Action Guide (*PAG*)

There is no uncertainty associated with a Protective Action Guide (PAG), so it will not be sampled from a distribution.

2.9 Plume External Dose Coefficient (*Pl_ExDC*)

Eckerman does not provide uncertainty information for plume external dose coefficients because the document was written in support of the SOARCA uncertainty analyses, in which "the dominant route of exposure…is exposure to contaminated ground surfaces" [6]. The Sequoyah SOARCA uncertainty analysis itself states that "cloudshine uncertainty is not treated because it is a relatively unimportant dose pathway compared with groundshine and inhalation" [7]. In a conversation with Eckerman on March 20, 2017, he recommended using the uncertainty for ground plane dose rate coefficients (described in Section 2.4) for the plume submersion dose coefficients.

2.10 Exposure to Dose Conversion Factor (*$XDCF_C$*)

FRMAC Assessment uses a chronic Exposure to Dose Conversion Factor ($XDCF_C$) of 1 as a measure of conservativism. This value is assumed to be fixed for this uncertainty analysis.

2.11 Weathering Factor (*WF*)

The Weathering Factor used by FRMAC comes from Anspaugh et al. [8]. No uncertainty information is given for this equation by Anspaugh.

Golikov et al. [13] use a log-normal fit for weathering in their study of external exposure in areas contaminated by the Chernobyl accident. The average of the time-dependent GSDs associated with the fit was 1.2. This GSD and a log-normal distribution will be used for weathering in this uncertainty analysis given a lack of uncertainty information in the Anspaugh paper.

2.12 Yield (Y_α, Y_β)

Alpha and beta yields are assumed to be well-characterized radioactive decay data with no associated uncertainty.

2.13 Summary of Assigned Input Distributions

Table 2. Summary of Public Protection DRL Input Distributions.

Input	Distribution Type	Mean	Standard Deviation	Mode	Lower Bound	Upper Bound	Units
Deposition Velocity	Triangular			0.3	0.03	3.0	cm/s
Breathing Rate – Light Exercise, Adult Male	Normal	1.75	0.42		0.540	3.00	m^3/hr
Breathing Rate – Activity-Averaged, Adult Male	Triangular			0.92	0.54	1.50	m^3/hr
Ground Roughness Factor	Normal	0.82	0.082				--
Resuspension Factor	Log-normal	NA*	4.2				--
Weathering Factor	Log-normal	NA*	1.2				--
Deposition External Dose Coefficient Multiplier	Triangular			0.8	0.5	1.5	--
Inhalation Dose Coefficient	Log-normal	17.3	1.5				mrem/µCi
Plume External Dose Coefficient Multiplier	Triangular			0.8	0.5	1.5	--

*Uncertainty on factors integrated over the time phase will be applied as a unitless multiplier using the variation presented in the literature

3 DATA COLLECTION SOURCES OF UNCERTAINTY

The health physics dose calculations are based on measured or projected concentrations of radionuclides in the environment. Measured values can be provided through multiple sources, including analytical laboratory results or field measurements obtained either through aerial measuring systems or ground-based monitoring teams. Projections are usually obtained from atmospheric modelling calculations performed using NARAC plume projections.

Sources of uncertainty in measurement values are discussed in this section. Sources of uncertainty from NARAC modelling projections are discussed in Section 4.

3.1 Laboratory Analysis

Based on the scenario defined for this project, an evaluation was conducted for the sources of uncertainly that could be identified and quantified for the laboratory sample analysis of ground deposition samples.

A discussion of the methodology employed by the FRMAC Lab Analysis regarding uncertainty is contained in the FRMAC Lab Analysis Manual, Appendix B [14]. The manual describes two principle factors that contribute to the overall uncertainty in sample analytical results: sample count time and background count rate according to the following equation:

$$\frac{\sigma_{R_{AAL}}}{R_{AAL}} = \left(\frac{R_{L_C}}{R_{AAL}}\right) * \frac{1}{k} * \sqrt{\left(\frac{R_{AAL}}{R_{L_C}}\right)\left(k\sqrt{\frac{1}{R_{BT_S}}}\right) + 1}$$

where:

$\frac{\sigma_{R_{AAL}}}{R_{AAL}}$ = relative uncertainty at the Analytical Action Level

R_{L_C} = count rate at the Critical Level (L_C)

R_{AAl} = count rate at the Analytical Action Level

R_B = background count rate

T_S = sample count time

k = normal deviate for a 1-sided confidence level (1.645 the 95% confidence level)

In this case, overall uncertainty is inversely proportional to both sample count time and background count rate. Thus, relatively high sample count times and background count rates would produce relatively low overall uncertainties. However, in practice, laboratories typically attempt to set up counting systems that minimize background count rates in order to attain the lowest possible detection levels. Nevertheless, both background count rate and sample count time are the key contributors to total uncertainty in measured sample activity.

For default ground deposition analyses, FRMAC requests laboratories to provide results that meet or are below a Critical Level (L_c) of 10% of the Analytical Action Level (AAL) determined by the FRMAC Assessment Scientists. In meeting this specified detection level, the relative uncertainty in the sample results are estimated to be ~10%. This estimate is based on a range of typical count times and background count rates. Table 3 demonstrates how the relative uncertainty at the AAL varies based on count time and background count rate.

Table 3. Relative Uncertainty Estimates at 10% of the Default Analytical Action Level.

Background count rate (CPM)	Sample Count Time (minutes)		
	1	10	100
.001	138%	78.2%	44.3%
1	25.4%	15.1%	11.1%
10	15.1%	9.9%	7.5%
100	9.9%	7.5%	6.6%

Given the amount of Cs-137 assumed for this scenario, the probability distributions for sample count time and background count rate are given in Table 4.

Table 4. Laboratory Analysis Sources of Uncertainty and Their Statistical Distribution.

Source of Uncertainty	Description of Uncertainty	Statistical Distribution
Sample count time (T_S)	As T_S increases, uncertainty decreases	Normal
Background count rate (R_B)	As R_B increases, uncertainty decreases	Normal

The parameters for the distribution of measured deposition activity can be derived using these characterizations given the amount of Cs-137 assumed for this scenario and assuming that typical collection procedures are followed. This derivation results in a normal distribution for the deposition value with a mean equivalent to the expected measurement of 330 μCi/m^2 of Cs-137 and a standard deviation of 0.17.

3.2 Field Monitoring

For the purposes of this project, the field monitoring portion of this process uses an on-site (in-situ) gamma spectroscopy measurement of radioactive material deposited on the ground.

3.2.1 Point Source Efficiency Calibration Uncertainty

Uncertainty in the point source efficiency calibration is derived from:

1. Uncertainty of the NIST traceable source activity,
2. Uncertainty of the detector efficiency for a point source, and
3. Uncertainty in the parameterization of the point source efficiency.

These uncertainties are not uncorrelated.

Uncertainty of the NIST traceable source activity is characterized as follows. The sources are measured at the manufacturers where the activity is determined by count rates compared to sources of known activity (surrogate sources). The uncertainties which are reported are a combination of the uncertainty of the known source and the counting statistics. The counting statistics can be made arbitrarily small by extending the counting time. Thus the uncertainty for the source activity reflects the uncertainty is the activity of the reference source. A uniform 3% uncertainty is thus assumed for the source activity.

Uncertainty of the detector efficiency for a point source is described as follows. NIST traceable point sources are measured at a fixed distance from the detector, and at multiple angles relative to the detector axis. The photopeak count rate is compared to the photon emission rate to determine the efficiency. The uncertainty is a combination of the counting statistics for the photopeak and the uncertainty on the activity of the source. The uncertainty from counting statistics is Gaussian and ranges from 0.3 to 3% depending upon the gamma ray emission rate and collection time.

Uncertainty of the parameterization of the point source efficiency is given as follows. The point source efficiency as a function of energy is fit to a polynomial so that it can be interpolated for intermediate energies. The uncertainty is measured as the fractional difference between the measured efficiency and the parameterization. The uncertainty follows a Cauchy distribution with a scale parameter of 0.02-0.025 (i.e., FWHM of 4-5%).

The assumed value for Cs-137 for this scenario will roll up these uncertainties into an overall measurement distribution.

3.2.2 Infinite Plane Source Efficiency Calibration Uncertainty

Uncertainty on the integral over the plane is characterized as follows. The point source efficiencies are weighted and summed over the angles relative to the detector axis. For simplicity the combined uncertainty for the point source efficiencies is assumed to be 6%, and is approximated by a Cauchy distribution. The uncertainty for the plane source efficiency will likely be a wider Cauchy distribution.

3.2.3 Infinite Plane Activity Uncertainty

Uncertainty of the peak area counts is described as follows. The activity is determined by multiplying the rate for counts in the photopeak area by the efficiency for an infinite plane source. The uncertainty for the counts in the peak is Gaussian.

4 NARAC Plume Predictions Sources of Uncertainty

This section documents the method used to quantify NARAC deposition plume uncertainty in relation to the project demonstration case study scenario. In Section 4.1, NARAC predicted air concentration uncertainty metrics developed using experimental data are discussed. Quantifying the impact of deposition processes uncertainty on predicted surface contamination is documented in Section 4.2. Final quantified NARAC plume uncertainty for the project scenario are summarized in Section 4.3. Concluding remarks are given in Section 4.4.

4.1 Benchmark Data

NARAC utilizes concentration measurements from atmospheric dispersion field experiments to compare with predicted values to determine model accuracy. Near-surface atmospheric tracer gas dispersion experiments range from constant winds over flat terrain with uniform vegetation cover (e.g., Prairie Grass Experiment; [15]) to highly variable wind fields in complex terrain along a coastline (e.g., Diablo Canyon Tracer Experiment; [16]). Based on the project demonstration case study scenario previously discussed, the Prairie Grass Experiment is the most relevant since it involves well resolved winds, uniform land cover and flat terrain. However, one caveat is that the experiment measured air concentration while the project scenario involves surface contamination uncertainty. As a result, the uncertainty associated with deposition processes will need to be quantified and integrated with the Prairie Grass NARAC benchmark results (discussed later in Section 4.2).

A metric useful for quantifying dispersion model accuracy is the ratio, r, of observed concentration values to predicted values at the same time and location. Statistics such as r are useful for comparing observed and predicted air and depositions concentration values that can range over several orders of magnitude. The equation for the concentration comparison metric r is given by:

$$r = \frac{observed\ value}{model\ predicted}$$

Based on the above equation, predicted concentration values within a factor of 2 of observations means $½ < r < 2$. For example, if an arbitrary concentration measurement is 1 ng/m^2, then both predicted values of 0.5 and 2 ng/m^2 are within a factor of 2 of the observed value.

The distribution of r values for NARAC simulations of the Prairie Grass tracer experiment are shown in Table 1 [17]. Roughly 50% of NARAC simulated air concentration values are within a factor of 2 of the observed value. Just over 80% of NARAC predicted values are within a factor of 10 of measured concentrations. Since the Prairie Grass experiment closely matches the project demonstration scenario, the comparison metric values provided in Table 5 are the best analog for quantifying NARAC CM product uncertainty for <u>air concentrations</u>. As a side note, observed to predicted concentration comparison metric values for the Diablo Canyon tracer experiment are also provided in Table 5 to illustrate the significant decrease in model accuracy when dispersion simulations occur in complex terrain with non-uniform wind fields.

Table 5. Distribution of NARAC observed to predicted concentration ratios for the Prairie Grass and Diablo Canyon tracer gas experiments.

Experiment	% *r* in factor 2	% *r* in factor 5	% *r* in factor 10
Prairie Grass	49	73	83
Diablo Canyon	18	41	56

4.2 Deposition Uncertainty

The model predicted concentration uncertainty values presented in Section 4.1 for the Prairie Grass experiment do not include error associated with deposition processes, which is needed for the project surface contamination scenario. NARAC has two methods for assigning a deposition velocity to a dispersion simulation to control the flux of airborne material to the surface. The first method is to use a fixed value that can be input by a subject matter expert as a function of meteorological conditions and surface characteristics. The second method utilizes high-resolution output from a numerical weather prediction model (when available) to parameterize meteorological and vegetation impacts to develop a grid cell specific deposition velocity.

Whether NARAC runs with a single fixed deposition velocity or one generate using sophisticated parameterizations, the accuracy is ultimately limited by the measurement error of observed deposition velocities. A literature review was conducted to determine the typical measurement error of dry deposition velocities for particles within the respirable range (0.1 to 10 µm) over grassland. The deposition velocity measurement error found in literature ranged from roughly 30 to 50% with an average of 40% [18], [19], [20], [21], [22], [23], [24].

To investigate the impact of the deposition velocity measurement error on predicted surface contamination concentrations, three experimental dispersion simulations were conducted. The first dispersion run used the default NARAC deposition velocity (0.3 cm/s) while the other two runs were performed with ± 40% of the default deposition velocity (i.e., 0.18 and 0.42 cm/s). Centerline surface contamination concentrations for the three dispersion simulations are shown in Figure 1.

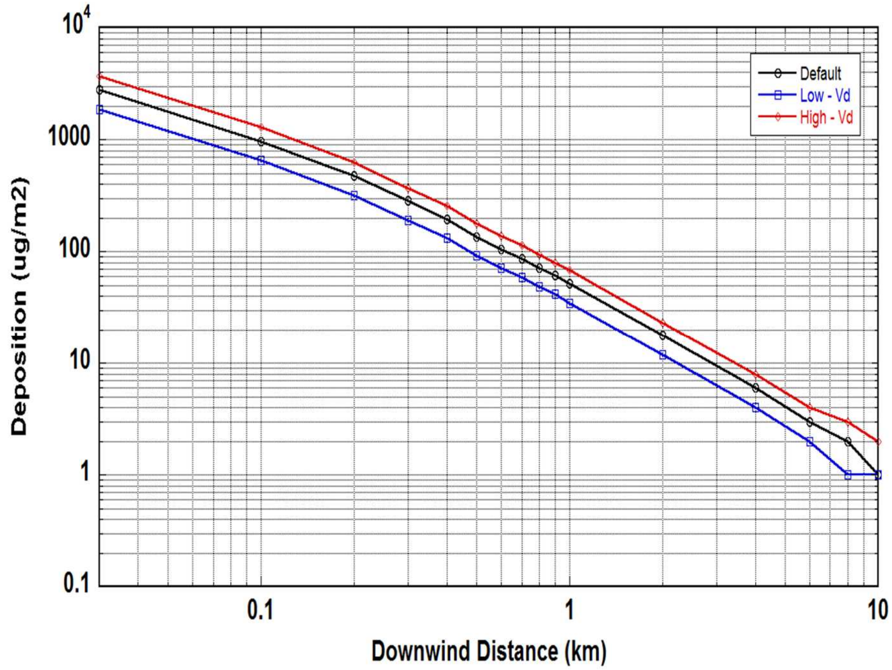

Figure 1. Centerline surface contamination concentrations for NARAC simulations using a default, high, and low deposition velocity.

Concentrations from the default deposition velocity run are shown in black while the low and high deposition velocity runs are shown in blue and red, respectively. From the release location out to a distance of around 10 km, the centerline deposition concentration difference between the default run and the high / low deposition velocity cases is on average around 32%.

4.3 Quantifying NARAC concentration uncertainty

A NARAC RDD dispersion simulation was made to generate scenario-dependent concentration uncertainty metrics (i.e., error mean and variance) based on the assumptions made for this project. The specifics of the RDD dispersion run are as follows:

- Source term: 1500 Ci of ^{137}Cs
- HE amount: 10 lbs of high explosive
- PSD: All particles with a size of 1 μm
- Meteorology: 4 m/s wind speed, no wind shear, neutral stability, no precipitation

As a point of reference, the RDD scenario results in a deposition concentration of 90.2 μCi m^{-2} at a distance of 1 km from the source location.

With predicted air concentration values provided by the RDD dispersion run, the next step in quantifying scenario dependent error metrics is to generate synthetic observations that will produce a NARAC r distribution similar to the Prairie Grass experiment (Figure 2).

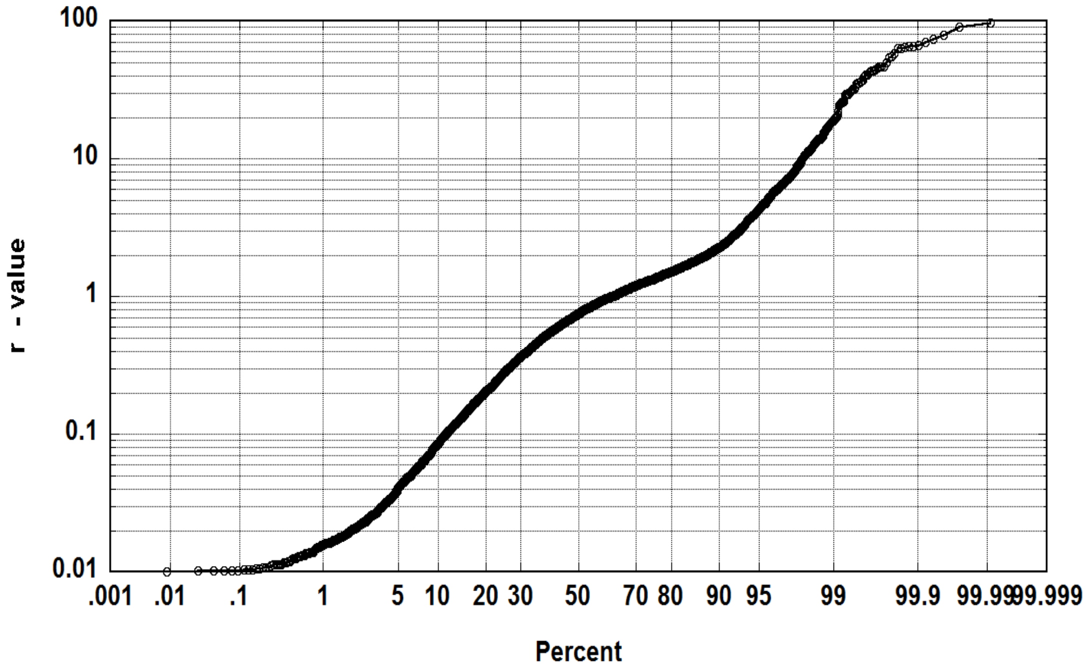

Figure 2. NARAC r value probability function for the Prairie Grass Experiment.

Consistent with NARAC operational procedures, Prairie Grass r value outliers that are more than two orders of magnitude greater or less than the median of the distribution were not included in the analysis. As a result, a total of 5711 individual r values are available in the Prairie Grass NARAC benchmark distribution. Next, the predicted 1-hour average air concentration plume following the RDD release was analyzed. Predicted concentrations along the plume edge (< 0.01 μCi m^{-3}) were removed from the analysis to avoid skewing statistics with extremely low concentration values. A synthetic concertation observation was then generated for each unique predicted concentration value (n=3505) by multiplying the predicted value by a r value randomly selected from the Prairie Grass distribution.

The final result of the analysis was a table of predicted and corresponding synthetic concentration observations specific to the project RDD scenario source term and PSD that has a r value distribution similar to NARAC model benchmarking tests using Prairie Grass Experiment measurements. A comparison of the predicted and synthetic concentration data results in a geometric mean (log form) of 0.616 and a geometric variance (log form) of 8.34. A log form of the error metrics is used since the concentration predictions span several orders of magnitude.

4.4 Conclusions

It is worth noting that the NARAC model uncertainty estimated for the simplified project RDD release scenario is on the low range of NARAC predicted concentration error. For example, the following key assumptions were necessary to quantify NARAC error for the project scenario:

- Meteorology is perfectly known
- RDD source term, geometry, and particle size distribution are perfectly known

- The Prairie Grass r value distribution for a continuous release is valid for a puff release (RDD scenario)

NARAC predicted concentration errors will be much larger for real world atmospheric releases where the source term and release mechanism are often poorly characterized. In addition, complex wind fields along coastlines and variable terrain and will significantly contribute to NARAC prediction error.

5 SUMMARY

The sources of error and uncertainty described for each part of the CM data product development process contribute to overall uncertainty in these data products. The identification of these sources of error and uncertainty is the first step in developing an understanding of this overall uncertainty. The characterization of these sources of error and uncertainty using probability distributions is the second step in this process and will allow each of these inputs to be sampled using a probabilistic framework that can be used to characterize uncertainty in the final CM data product.

6 REFERENCES

[1] *Federal Radiological Monitoring and Assessment Center (FRMAC) Assessment Manual, Volume 1 Overview and Methods*, SAND2015-2884 R, Sandia National Laboratories, Albuquerque, NM, 2015.

[2] *Evaluation of Severe Accident Risks: Quantification of Major Input Parameters*, NUREG/CR-4551, Vol. 2, Rev. 1, Part 7, U.S. Nuclear Regulatory Commission, Washington, DC, 1990.

[3] *Human Respiratory Tract Model for Radiological Protection,* ICRP Publication 66, International Commission on Radiological Protection, Ottawa, Ontario, Canada, 1994.

[4] *Development of Probabilistic RESRAD 6.0 and RESRAD-BUILD 3.0 Computer Codes*, NUREG/CR-6697, ANL/EAD/TM-98, Argonne National Laboratory, Argonne, IL, 2000.

[5] *Exposure Factors Handbook*, EPA/600/R-090/052F, U.S. Environmental Protection Agency, Washington, DC, September 2011.

[6] Eckerman, K., *Radiation Dose and Health Risk Estimation: Technical Basis for the State-of-the-Art Reactor Consequence Analysis Project*, Oak Ridge National Laboratory, Oak Ridge, TN, 2012.

[7] *State-of-the-Art Reactor Consequence Analysis (SOARCA) Project, Sequoyah Integrated Deterministic and Uncertainty Analysis Draft Report*, ML16096A374, Sandia National Laboratories, Albuquerque, NM, 2017.

[8] Anspaugh, L. R., et al., "Movement of Radionuclides in Terrestrial Ecosystems by Physical Processes" in *Health Physics*, Vol. 82, pp. 670-679, April 2002.

[9] Likhtarev, I.A., Kovgan, L.N., Jacob, P., Anspaugh, L.R., "Chernobyl Accident: Retrospective and Prospective Estimates of External Dose of the Population of Ukraine" in *Health Physics*, Vol. 82, pp. 290-303, 2002.

[10] Beck, H.L., *Exposure Rate Conversion Factors for Radionuclides Deposited on the Ground*, EML-378, U.S. Department of Energy Environmental Measurements Laboratory, New York, NY, 1980.

[11] *MELCOR Accident Consequence Code System (MACCS) User's Guide and Reference Manual Draft Report*, Sandia National Laboratories, Albuquerque, NM, 2017.

[12] Maxwell, R. and Anspaugh, L., "An Improved Model for Prediction of Resuspension" in *Health Physics*, Vol. 101, pp. 722-730, December 2011.

[13] Golikov, V.Y., Balonov, M.I., Jacob, P., "External Exposure of the Population Living in Areas of Russia Contaminated Due to the Chernobyl Accident" in *Radiat Environ Biophys*, Vol. 41, pp. 185-193, 2002.

[14] *Federal Radiological Monitoring and Assessment Center (FRMAC) Laboratory Analysis Manual*, Appendix B, SAND2013-10382P, Sandia National Laboratories, Albuquerque, NM, December 2013.

[15] Barad, M.L., “Project Prairie Grass, a field program in diffusion” in *Geophys. Res. Pap. 59*. Air Force Cambridge Centre, 1958.

[16] Thuillier, R.H., “ Evaluation of a Puff Dispersion Model in Complex Terrain” in *Journal of the Air & Waste Management Association*, 42:3, 290-297, 1992.

[17] Foster, K.T., G. Sugiyama, J.S. Nasstrom, J.M. Leone, Jr., S.T. Chan, and B.M. Bowen, “The use of an operational model evaluation system for model intercomparison” in *Int. J. Environment and Pollution*, 14, 77-88, 2000.

[18] Clough, W. S., “The deposition of particles on moss and grass surfaces” in *Atmospheric Environment* 9, 1113-1119, 1975.

[19] Garland, J.A., “Field measurements of the dry deposition of small particles to grass” in *Deposition of* Atmospheric Pollutants, H.W.Georgii and J.Pankrath (Eds.) D. Reidel, Oberursel/Tanus, West Germany, 9–16, 1981.

[20] Garland, J.A., “Dry deposition of small particles to grass in field conditions” in *Precipitation Scavenging, Dry Deposition and Resuspension*, H.R. Pruppacher, R.G. Semonin, W.G.N. Slinn (Eds.), Elsevier, Amsterdam (1983), pp. 849–857, 1983.

[21] Wesely, M.L., D.R. Cook, R.L. Hart, B.B. Hicks, J.L. Durham, R.E. Speer, O.J. Stedman, R.J. Tropp, “Eddy correlation measurements of the dry deposition of particulate sulphur and submicron particles” in *Precipitation Scavenging, Dry Deposition and Resuspension*, H.R. Pruppacher, R.G. Semonin, W.G.N. Slinn (Eds.), Elsevier, Amsterdam, pp. 943–952, 1983.

[22] Wesely, M.L., D.R. Cook, R.L. Hart, R.E. Speer, “Measurements and parameterization of particulate sulfur dry deposition over grass” in *Journal of Geophysical Research*, 90, pp. 2131–2143, 1985.

[23] Duan, B., C.W. Fairall, D.W. Thomson, “Eddy correlation measurements of the dry deposition of particles in wintertime” in *Journal of Applied Meteorology*, 27, pp. 642–652, 1988.

[24] Allen, A.G., R.M. Harrison, K.W. Nicholson, “Dry deposition of fine aerosol to a short grass surface” in *Atmospheric Environment*, 25A, pp. 2671–2676, 1991.